How policy failure and power relations drive COVID-19 pandemic waves: A control theory perspective

Rodrick Wallace

How policy failure and power relations drive COVID-19 pandemic waves: A control theory perspective

Rodrick Wallace
The New York State Psychiatric Institute
rodrick.wallace@gmail.com, rodrick.wallace@nyspi.columbia.edu

May 2, 2021

Abstract

Elementary control theory and epidemic spread models illustrate the deadly impacts delay in recognizing pandemic threat and failure of institutional cognition in facing that threat can have on the institutions of public health. While short delays may cause some oscillation that rapidly dies out, sufficiently large time gaps trigger multiple infection waves of increasing severity, much like the onset of a power network blackout or of uncontrollable vehicle fishtailing. Similar – and synergistic – oscillations are found to be triggered by sufficiently low rates of institutional cognition. This approach begins to lift the cultural constraints inherent to host-pathogen population dynamics models of infectious disease in social systems sculpted by the synergisms of geography, power relations, and path-dependent historical trajectory.

Key Words: cultural constraint, epidemic disease, control theory, delay, institutional cognition, mathematical models, power relations, public policy,

1 Introduction

Very few polities have, like New Zealand and Singapore in figure 1, after the initial surge, succeeded in suppressing pandemic COVID-19.

Others either did not act promptly, or failed to act consistently, and, like the United States, Brazil, and England within the UK, and South Africa have suffered recurrent, and even growing waves of infection. See figure 2.

Here, we will study the patterns of figures 1 and 2 from a perspective somewhat removed from currently-fashionable host-pathogen population dynamics. A first alternate perspective is that of control theory, in the context of an inherently unstable system where the control impulse is further burdened by increasing response delay. Castro et al. (2021) provide a somewhat different view of the ongoing Brazilian catastrophe.

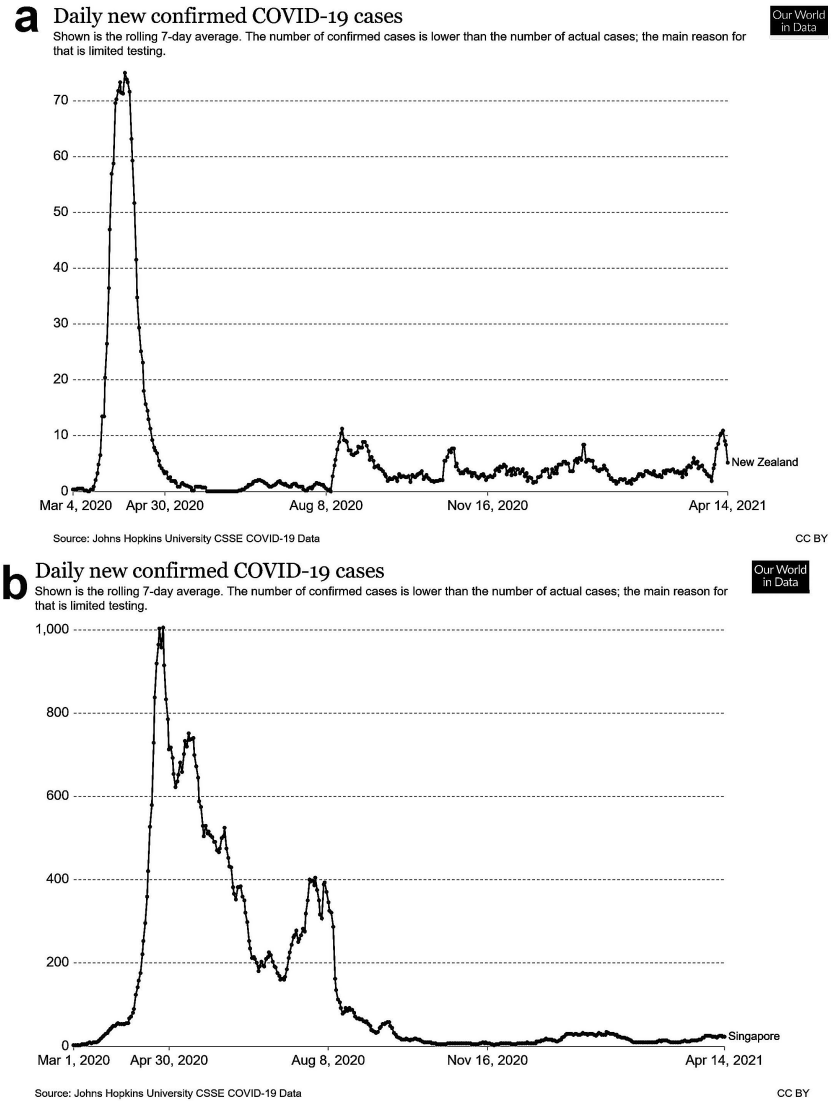

Figure 1: From Johns Hopkins (2021). (a) Number of confirmed COVID-19 cases in New Zealand, 3/1/20-3/8/21. (b) COVID-19 cases for Singapore. Control measures were promptly imposed, consistently maintained, and succeeded.

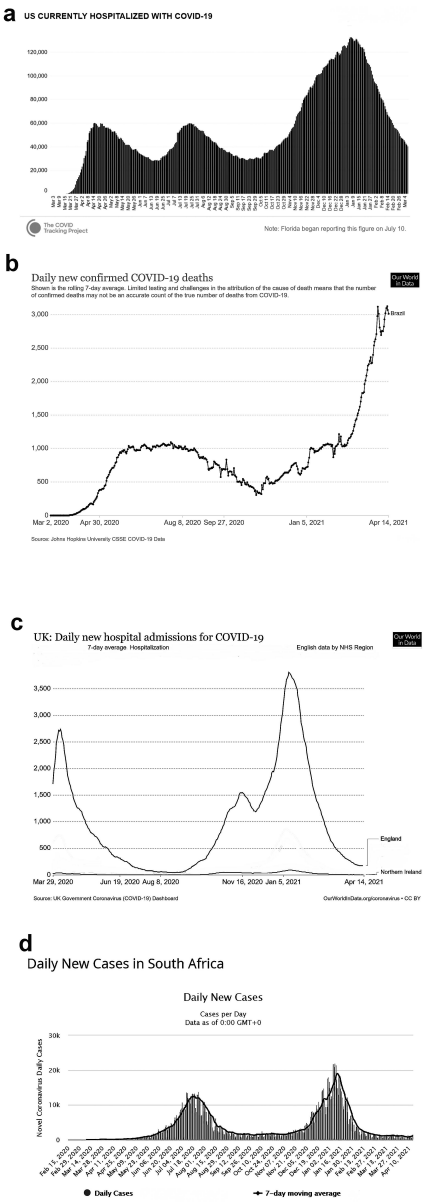

Figure 2: (a) From Covid Tracking Project (2021). COVID-19 hospitalizations in the USA over the same period as figure 1 show increasing amplitude instability consistent with critical delay in problem recognition and address. (b) From Our World in Data, via Johns Hopkins, reported COVID-19 deaths in Brazil, March 2020 through April 14, 2021. Again, increasing amplitude oscillations. (c) Adapted from Our World Data. COVID-19 hospitalizations in England and Northern Ireland from NHS data. Yet again, oscillation of increasing amplitude. (d) Reported cases for South Africa.

The delay/instability problem in control dynamics has been of central concern outside epidemiology and public health. Ali et al. (1997) describe at some length how time delay in active control systems causes unsynchronized application of the control forces, and shows how this unsynchronization not only degrades the system performance, but also causes severe instability in system response.

For individual human cognition, one can invoke the example of Delayed Auditory Feedback (DAF) in which an artificially-induced delay of about 175ms between speech and hearing triggers extreme stress (e.g., Yates 1963).

The perspective extends to failure in disease control, and there are fundamental cultural reasons for a significant reorientation.

Epidemiologists in Western nations, as a consequence of powerful and deeply-held cultural mechanisms, will usually focus on the 'salient object' (Nisbett et al. 2001) of the population dynamics seen as the 'fundamental' linkage between host and pathogen. This perspective is currently most saliently instantiated by the simplistic 'R-zero' model (e.g., Bailey 1975; Wallace and Wallace 2016), as follows.

Let X, Y, Z be, respectively, susceptible, infective, and 'removed' – dead or immune – subpopulations, with $N = X + Y + Z =$ constant. The Kermack-McKendrick model of infectious disease is as follows:

$$\begin{aligned} dX/dt &= -\beta XY \\ dY/dt &= (\beta X - \gamma)Y \\ dZ/dt &= \gamma Y \\ Y_\infty &= 0 \\ Z_\infty &= \frac{L_W\left(-\frac{\beta}{\gamma}\exp[-\frac{\beta}{\gamma}N]\right)}{\beta/\gamma} + N \end{aligned} \tag{1}$$

where L_W is the $n = 0$ order Lambert W-function that satisfies the relation

$$L_W(n, x)\exp[L_W(n, x)] = x$$

This function will appear repeatedly below. Except for $n = 0, -1$, $L_W(n, x)$ is complex valued. It is real valued for $n = 0$ in the range $-\exp[-1] < x < \infty$, and for order $n = -1$ over the range $-\exp[-1] < x < 0$.

Taking the initial infected population at time zero to be $Y_0 > 0$, if the 'reproduction number' $R_0 \equiv \beta X_0/\gamma < 1$, the infection will decline and become (at least locally) extinct. There are many variations, of differing complexity, and some have been used for policy purposes during the COVID-19 pandemic (e.g., Ferguson et al. 2020). Shayak et al. (2021), for example, apply a delay-differential equation (DDE) version to explore the impact of reproduction number on the multiwave spreading dynamics of COVID-19 with temporary immunity.

A different, and in our view, more sophisticated, approach is taken by Pedro et al. (2020). They examine in some detail the interplay between disease dynamics and social processes as follows.

> A second wave of COVID-19 is widely feared... as many jurisdictions around the world begin lifting restrictions that have held viral transmission in check. To address this issue, we analyzed [the] ... interplay between SARS-CoV-2 transmission dynamics and social dynamics concerning public support for physical distancing and school and workplace closure ... [finding] that a second wave of COVID-19 (and sometimes also a third wave) was likely... In some cases, the second peak was higher than the first peak...
>
> Time delays... destabilize dynamics... and we... suspect that a model extension including a response to lagged outcomes... would exacerbate the severity of second waves...

Pedro et al. (2020) conclude that because interactions between the dynamics of disease spread and social processes will play a major role in shaping the pandemic, more effort in transmission modeling of COVID-19 should be devoted to accounting for them.

We will focus even less on the 'salient object' of individual-oriented disease population dynamics, and bear down heavily on the larger embedding contexts of geography and path-dependent historical trajectory reflecting the power relations defining and sculpting the modern state and its subservient public health institutions. Nisbett et al. (2001) provide deeper exploration of the implications of such refocs.

As Wallace and Wallace (2016 Ch. 4) studied similar matters in the context of the West African Ebola outbreaks, finding that

> Modern states are cognitive entities. Faced with dynamic patterns of threat or affordance – like spreading infection – national states or international confederations and their socioeconomic subcomponents must, can, and do choose a smaller set of responses from a much larger domain of those possible to them. Such choice... reduces uncertainty and [this] implies the existence of an information source generating successive [disease control] messages. That is, modern states are cognitive...

Pandemic propagation is not constrained by the 'salient object' of the R_0 model of Eq.(1). Infection spreads, like water through cracks in ice, along a social geography reflected by the modes of governance and their defining – and sometimes hidden – power relations. Figure 3, adapted from Abler, Adams and Gould (1971), characterizes the three levels of disease spread that have operated since mercantile traffic became routine.

The top plane shows *hierarchical diffusion* from larger to smaller metropolitan regions along air, rail, road, and river travel patterns. As with COVID-19,

small outlying outbreaks become entrained into the peak of the urban hierarchy, and then blow back down the hierarchy through routine travel patterns.

The second plane characterizes *spatial contagion* , driven by the daily journey-to-work from central cities back and forth to their outlying suburbs.

The third plane, local, represents *network diffusion* , person-to-person spread in homes, schools, workplaces, retail enterprises, and 'superspreader' social events.

In sum, spatial diffusion of both information and infection within a modern polity is networked by travel patterns at and across the various and different scales and levels of organization.

For application of this perspective to the 'slow plague' of HIV/AIDS in the USA, see Gould (1993), Gould and Wallace (1994), and Wallace et al. (1997, 1999). D. Wallace and R. Wallace (2020, Ch. 3) apply similar ideas to the spatial diffusion of COVID-19 in the New York Metropolitan Region.

Figure 4, from Wallace et al. (1999), a study of AIDS across the 25 largest US metropolitan regions, makes clear the overwhelming dominance of the New York Metropolitan Region in the dynamics of the country's pattern of infectious disease spread: as goes New York City, ultimately, so goes the entire nation. AIDS is, to reiterate, a 'slow plague' in the sense of Gould (1993), since any rapid dynamics analogous to those of figures 1 and 2 are smoothed out by the sometimes decade-long asymptomatic but infectious period of HIV.

Figure 4 shows the log of reported AIDS cases in the 25 largest US metropolitan regions for two time periods, through April, 1991, and from April, 1991 through June, 1995. The New York Metropolitan Region is the point on the upper right of the graph.

The log of reported AIDS cases is expressed as a function of the logs of (1) the number of reported violent crimes for 1991, (2) the log of the ratio of manufacturing employment jobs for 1987 and 1972 – an index of boom town/bust town dynamics – and, (3) the log of the probability of contact with the New York Metropolitan Area, measured in terms of 1985-1990 interregional and intraregional migration. Multivariate analysis of covariance (MANCOVA) shows that, as the New York Metropolitan Region rose in AIDS cases, it pulled up AIDS cases in a cascade across the remaining 24 of the country's largest regions.

Again, as goes New York City, so goes the nation, in terms of emerging infection.

In the USA, public health response to the perturbation of a spreading infection is organized as a large, crosslinked, institutional network, at the national, state, large urban center, and county levels and scales of organization. There are, unfortunately, no general metropolitan regional-scale public health institutions, a central omission driven by local histories of racial segregation, i.e, the current evolutionary incarnation of the nation's 'peculiar institution'.

Here, we will be particularly interested in the modalities of governance and the dynamics of their response to a pandemic 'perturbation'. Our central focus will be on the impact of delays in effective institutional response to disease onset.

Think about this for a long minute.

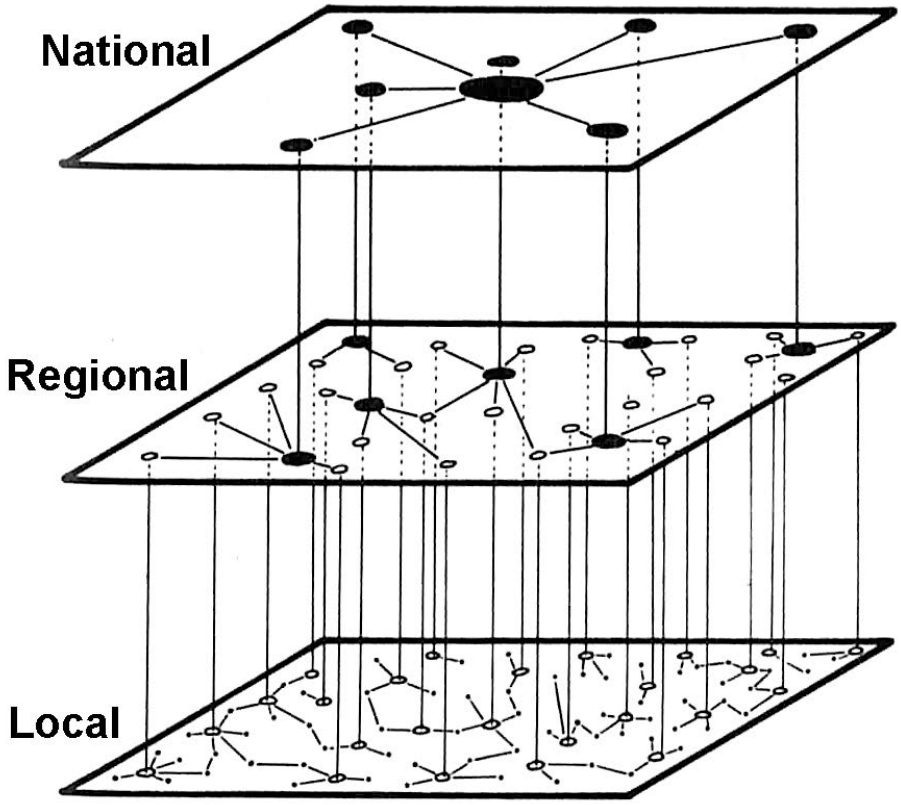

National, regional, and local planes of diffusion.

Figure 3: Adapted from Abler, Adams and Gould (1971). National spread of a contagious process. The top plane represents hierarchical diffusion. Infection is first entrained into the largest central city, where it incubates within marginalized populations, and then blows down the urban hierarchy along air, rail, and highway travel paths to other large cities. The central plane represents spatial contagion, the spread from central cities throughout the metropolitan region by the daily journey-to-work. The lowest level represents network diffusion, between individuals within families, workplaces, and ordinary social contacts. Policies must be crafted according to scale and level of organization to stop contagious spread.

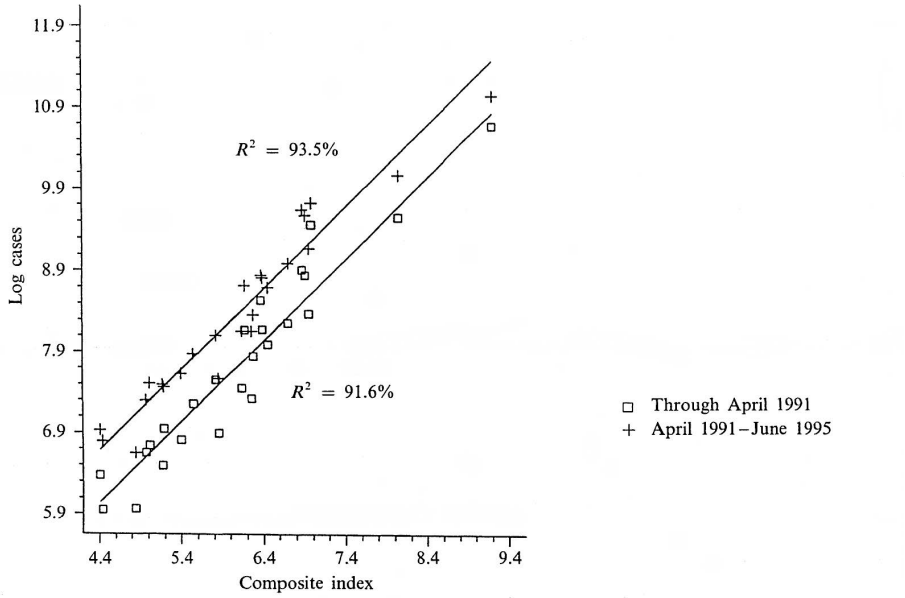

Multivariate analysis of covariance for log AIDS cases, through April 1991, and for the period April 1991–June 1995. The composite index is $X = 0.764 \log(\text{USVC91}) + 0.827 \log(\text{USME87}/\text{USME72}) + 0.299 \log(\mathbf{P}[1;])$. The two lines are highly parallel but have significantly different intercepts.

Figure 4: Adapted from Wallace et al. (1999). AIDS spread across the 25 largest metropolitan regions of the US. Infectious disease dynamics in the US are strongly dominated by what happens in the apex of the US urban hierarchy, the New York Metropolitan Region, the uppermost points on the graph.

In more detail, we explore two relatively simple models of epidemic spread from this top-down perspective. The first applies recent results from control theory to delayed intervention, and the second reexamines a simplified version of the 'R_0' model under the influence of lagged official response. We will end with an exploration of left-weighted distributed response delay that can be considered as institutional cognition rate.

2 Control system dynamics

The Data Rate Theorem

Consider a powerful car driven at high speed on a twisting roadway at night. The driver's own response time to twists in the road is convoluted with responsiveness of both steering and brakes, the brightness of the car's headlamps, all in tightly-coupled synergism with the inherent 'twistiness' of the road itself. This gestalt, in its totality, determines the probability of safe completion of the trip. This gestalt dynamic can be made formal through Control Theory's Data Rate Theorem (Nair et al. 2007).

Institutions facting rapidly changing environments, like the fast car on a twisting road, are inherently unstable, since the 'roadway' on which they operate can always run them into a ditch.

The Data Rate Theorem (DRT) of control theory determines the minimum rate at which control information must be imposed for an inherently unstable control system to remain stable.

The standard analysis makes a linear expansion of system dynamics near the control system's nonequilibrium steady state (nss). Assume there is an n-dimensional vector of parameters at time t, x_t that sufficiently characterizes the system. The state at time $t+1$ is then assumed to be determined by the first-order relation

$$x_{t+1} = \mathbf{A}x_t + \mathbf{B}u_t + W_t \tag{2}$$

$\mathbf{A}$ and $\mathbf{B}$ are fixed n-dimensional square matrices. u_t is a vector of the control information. W_t an n-dimensional vector of Brownian 'white' noise.

Figure 5 presents a minimal structure for a command-and-control process influenced by that 'noise'.

The Data Rate Theorem – an adaptation of the Bode Integral Theorem – states that, if H is the rate at which control information is provided sufficient to stabilize an inherently unstable control system, it must be greater than a minimum, H_0, given as

$$H > H_0 \equiv \log[|\det[\mathbf{A}^m]|] \tag{3}$$

det is the determinant of the matrix $\mathbf{A}^m$, with $m \leq n$, taking $\mathbf{A}^m$ is the subcomponent of $\mathbf{A}$ with eigenvalues ≥ 1. The right hand side of Eq.(3) is characterized as the rate at which the unstable system itself generates 'topological information'.

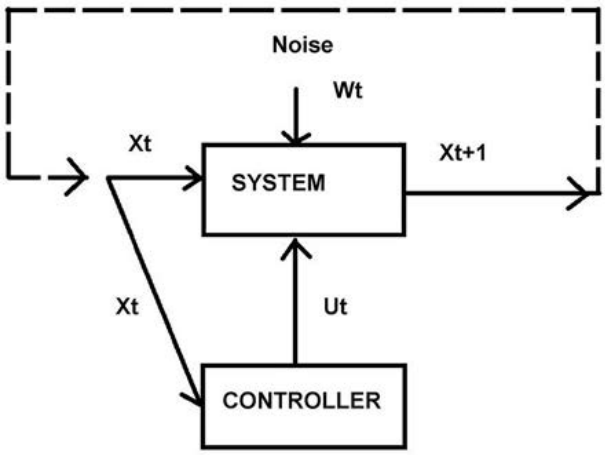

Figure 5: The state of a system, X, is compared with what has been ordered, and, on detection of 'error', a corrective control signal U is sent at an appropriate rate, against the influence of a noise W. The rate of transmission of that control signal information must exceed the rate at which the inherently unstable system generates it's own 'topological information'.

The system becomes uncontrolable if this inequality is violated. For the speeding vehicle example, if headlights go out, or if the steering becomes unreliable, a twisting roadway cannot be navigated, no matter how powerful the engine or how skilled the driver.

In the context of a nation's public health, a set of interlinked institutions must generate control information at and across the various scales and levels of organization of figure 3 at a rate greater than the infection itself is generating topological information by spreading down the urban hierarchy, from central city to suburb, and from person to person.

This is a harsh demand, not at all unlike that facing the Red Army on June 22, 1941.

The effect of delay

There are different delays in public health response to a suddenly emerging infection. The most obvious is the time it takes to implement a new policy against inherent institutional inertia. We will treat such delay using an 'exponential' model for the control information rate H being sent out by the public health establishment across the different scales and levels of organization of the underlying polity, so that

$$dH(t)/dt = \beta - \alpha H(t)$$

$$H(t) = \frac{\beta}{\alpha}\left(1 - \exp[-\alpha t]\right)$$

$$H(t) \to \frac{\beta}{\alpha} \tag{4}$$

This generates an 'inverted-J' curve that tops out at $H = \beta/\alpha > H_0$ at a rate determined by α.

There is a second kind of delay.

Suppose there is a significant lag, say δ, in the time it takes to actually recognize – or admit – a threat, so that

$$dH/dt = \beta - \alpha H(t - \delta) \tag{5}$$

Solving a simple differential-delay equation can be done by seeking a solution in terms of an 'integrating factor' s, so that

$$H_s(t) = \frac{\beta}{\alpha}\left(1 - \exp[st]\right) \tag{6}$$

This generates a characteristic equation whose solution is

$$s = \frac{L_W(n, -\alpha\delta)}{\delta} \tag{7}$$

where, again, L_W is the Lambert W-function of order n.

Taking $n = -1$, $\alpha = 1$, figure 6 shows the real and complex values of s as $\alpha\delta > 0$ increases.

In view of Eq.(6), the range of $\alpha\delta$ for which the complex component of s is zero is important, since it determines the limit above which oscillation sets in. Recall that $L_W(-1, x)$ is real only for $-\exp[-1 < x < 0$ and that the real part of $L_W(-1, -z)$ becomes positive for $z > \pi/2$. Hence the condition for a non-oscillating response is that $\alpha\delta < \exp[-1] \approx 0.3679$. Response delay, increasing $\alpha\delta$, stretches out the time over which $H(t)$ tops out, as in figure 7. Here, $\alpha = \beta = 1$. The shorter delay is $\delta = 0.25$ and the longer $\delta = \exp[-1]$.

Figure 8 examines the real values of $H_s(t)$ for $\alpha\delta$ just to the left and right of the point where the real component of s changes sign, from negative to positive, here at $\alpha\delta \approx 1.59$, again taking $\alpha = \beta = 1$. For $\alpha\delta$ below that value, the system 'rings' slightly before settling down. For delays above that value, the system begins 'hunting', i.e., to overcorrect, then to overcorrect again, until, as it were, the speeding vehicle runs off the road. A negative value of $Re[H(t)]$ indicates complete collapse.

The Lambert W-function always suggests – perhaps even mandates – some underlying formal network. Newman (2010), Spenser (2010) and Yi et al. (2010, 2011, 2012) provide discussion and examples. Yi et al. (2012) explicitly use Lambert W-functions to solve delay differential equations, including extending results to multidimensional systems via the matrix Lambert W-function.

Discussion of delay-differential equations like Eq.(5) can be found in Lou and Sun (2011) and many other standard references.

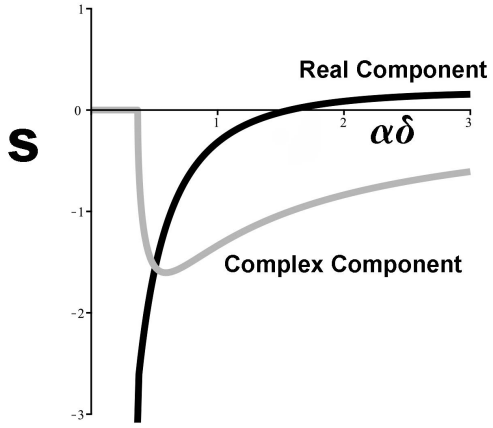

Figure 6: The exponential 'integrating factor' s replaces α in Eq.(9.6). There are two critical values of the delay δ, derived from the appearance of the Lambert W-function. The first is at the point where the complex component becomes nonzero, representing the onset of dying oscillatory dynamics. The second is the point at which the real component of s becomes greater than zero, implying explosive growth in oscillations. Recall that the real part of $L_W(-1, -z)$ becomes positive for $z > \pi/2$. Note that the periodicity, determined by the magnitude of the complex component, changes as $\alpha\delta$ increases beyond the first critical point.

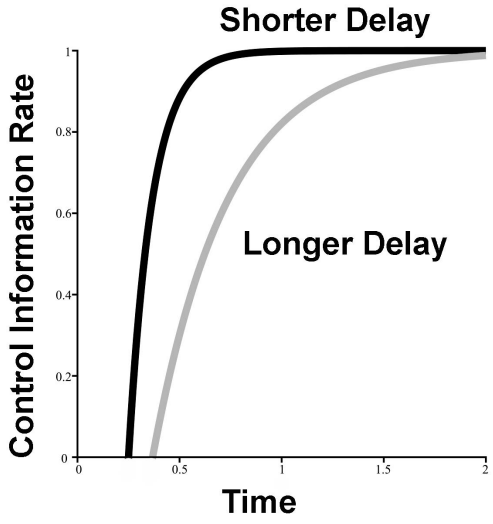

Figure 7: Control information rates when $\alpha\delta$ is below the first critical value at fixed α. Rising delay slows the rate of increase of H_s.

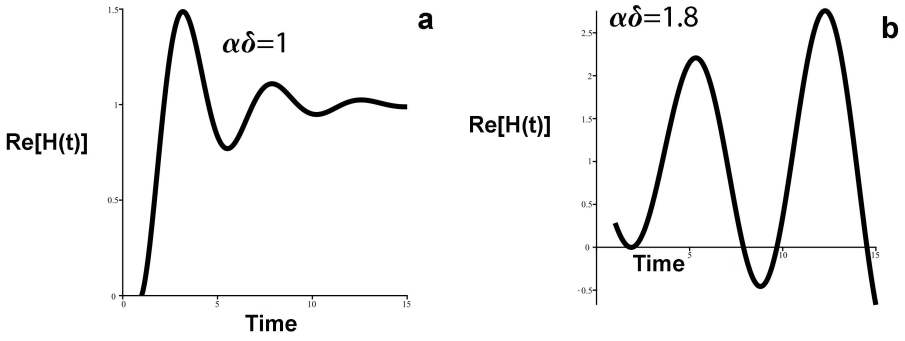

Figure 8: (a) Ringing of $Re[H(t)]$ when $\alpha\delta$ is between critical points. (b) Unstable hunting dynamics of $Re[H(t)]$ when δ exceeds the second critical value. According to this model, at $\alpha\delta = 1.8$, the real part of $H(t)$ reaches negative values on the downswing, indicating complete collapse of control.

Following Mao et al. (2005), we make stochastic extension of Eqs.(6) and (7) by observing that

$$dH_s/dt = s(H_s(t) - \beta/\alpha) \tag{8}$$

This leads directly to a stochastic differential equation (Protter 2005)

$$dH_t^s = s(H_t^s - \beta/\alpha)dt + \sigma H_t^s dW_t \tag{9}$$

Here, dW_t is assumed to be ordinary Brownian noise, so that the second term represents volatility of magnitude σ.

Applying the Ito Chain Rule (Protter 2005) to $(H_t^s)^2$ gives the variance as

$$Var(H^s) = \left(\frac{s\beta/\alpha}{\sigma^2/2 + s}\right)^2 - \left(\frac{\beta}{\alpha}\right)^2 \tag{10}$$

As above, variance becomes grossly unstable – complex – if $\alpha\delta > \exp[-1]$. That is, as expected, delay can badly exacerbate inherent stochastic instabilities afflicting control systems. Even if this condition is not violated, a sufficiently large value of σ will trigger an explosive variability, since s must be both negative and real for system stability.

3 Infection dynamics

Another approach to the dynamics of delay is via the number of infected individuals at the earliest stage of the pandemic, when there have been few if any 'removals'. Then, according to Eq.(1), $dY/dt \approx aY(t)$, $a \equiv (\beta X - \gamma) > 0$ so that $Y(t) \approx Y_0 \exp[at]$, i.e, exponential growth early on, in the context of a

constant influx of infectives from surrounding areas, or via other random events, at a rate β.

Typically, in 'advanced' nations, there should be a robust public health response at the earliest stage of the pandemic, so that

$$dY/dt \approx \beta + aY(t) - bY(t-\delta)$$
$$b > a > 0 \tag{11}$$

If there is no delay in robust public health response, so that $\delta = 0$, then some calculation finds, taking $Y(t=0) = Y_0$ and, again, assuming $b > a > 0$,

$$Y(t) = \frac{\beta}{b-a} - \frac{[\beta - Y_0(b-a)]\exp[-(b-a)t]}{b-a}$$
$$Y(0) = Y_0 \rightarrow \frac{\beta}{b-a} \tag{12}$$

The pandemic does not propagate, but settles in to a low level endemic state, depending on the influx rate β.

What, here, is 'δ'? Delay in response, as Pedro et al. (2020) indicate, may involve lagged outcomes like reported cases but, as we have seen recently with regard to COVID-19 in the USA and elsewhere, includes executive misfeasance, malfeasance, and nonfeasance ranging across dithering, denial, incompetence, outright lying, and crony profiteering, structured according to preexisting power relations across the polity. In consequence, δ can become quite large. What then?

Using the approach of Eq.(6), we can seek a solution $Y(t)$ under finite delay δ as having the same form as Eq.(12), but replacing the term $-(b-a)t$ in the exponential with st. Then, a very similar characteristic equation calculation gives

$$s = \frac{a\delta + L_W\left(n, -b\delta\, \mathrm{e}^{-a\delta}\right)}{\delta} \tag{13}$$

Figure 9 shows Eq.(13), taking $n = -1$, $a = 1$, $b = 2$. It is, not surprisingly, quite close to figure 6, and the subsequent arguments are similar.

The condition for zero complex component, however, is a little more complicated,

$$b\delta \exp[-a\delta] < \exp[-1] \tag{14}$$

Figure 10 displays $Y(t)$ for two delays within that range, taking $\beta = 1, Y_0 = 20, a = 1$, $b = 2, \delta = 0.1, 0.2$. The longer delay slows decline of infection to a low endemic level.

Again, figure 9 identifies two critical values for δ, the first determining onset of oscillatory dynamics, and the second, when the real component becomes positive, determining explosive, oscillating, growth of infection in spite of the

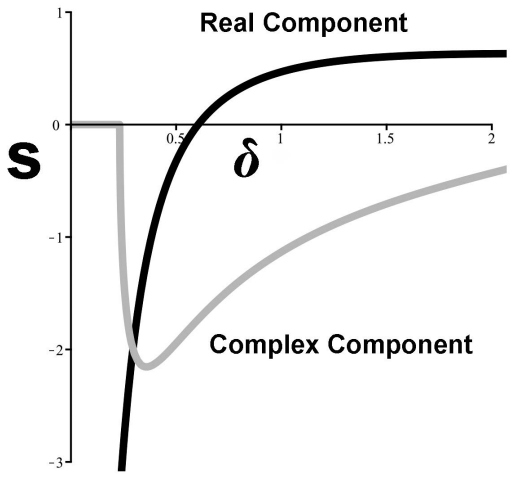

Figure 9: Form of Eq.(13) for $n = -1, a = 1, b = 2$. Not surprisingly, the same critical behaviors as in figure 6 are driven by increases in delay δ. Recall again that the real part of $L_W(-1, -z)$ becomes positive for $z > \pi/2$.

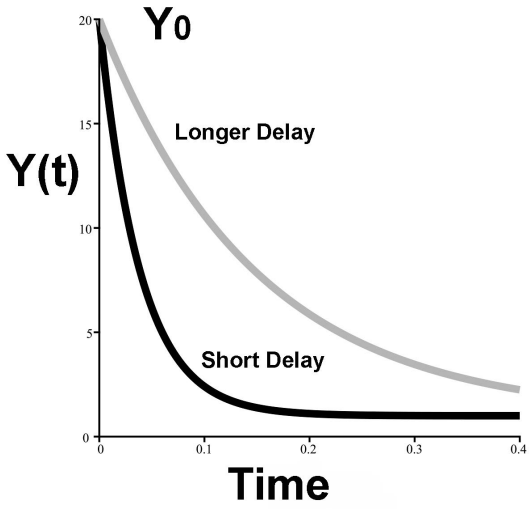

Figure 10: Number of infectives vs. time for delays $\delta = 0.1,\ 0.2$, within the real-valued range of figure 9. Here, $n = -1, \beta = 1, a = 1,\ b = 2, Y_0 = 20, \delta = 0.1,\ 0.2$. This is, in effect, the inverse of figure 7. Delay prolongs infection. Sufficient delay produces oscillating explosive growth of infection similar to figure 8, in spite of a robust public health response.

condition $b > a > 0$ which, in the absence of delay, drives the infection to low endemicity.

The stochastic DDE analysis, here in terms of the Ito Chain Rule applied to $Y(t)^2$ shows again that sufficient delay will grossly destabilize disease control dynamics. Taking $Y(t)$ as in the argument leading to Eq.(13) gives the SDE

$$dY_t = s[Y_t - \frac{\beta}{b-a}]dt + \sigma Y_t dW_t \tag{15}$$

Application of the Ito Chain Rule in second order shows

$$< Y_t^2 > \approx \left(\frac{s\beta}{(\sigma^2/2+s)(b-a)}\right)^2 \tag{16}$$

Sufficiently large σ will overcome the negative real part of s in figure 9, leading to explosive instability in variance well before the second critical point. Similarly, if $a \to b$, variance explodes.

4 Distributed delay – cognition rate models

The generalization of Eq.(5) to distributed delay takes the form

$$dH/dt = \beta - \alpha \int_0^t H(t-\tau) f(\tau) d\tau \tag{17}$$

where $\int f(\tau)d\tau = 1$. If f is a Dirac delta function in $(\tau - \delta)$, then we fully recover Eq.(5). If $f(\tau)$ is symmetric and sharply peaked at some delay, then dynamics will again be similar. Bernard et al. (2001) show, for differential delay equations, that distributions concentrated to the left show greater stability to parameter variations, and we will model attention span using the exponential distribution, which is heavily left-loaded: $f(x) = m \exp[-mx]$.

Taking $H(0) = 0$, applying the Laplace transform to Eq.(17) gives

$$\mathcal{L}(H(t), t, s) = \frac{\beta}{s(\alpha \mathcal{L}(f(t), t, s) + s)} \tag{18}$$

Using the exponential distribution of mean m, calculation and inversion of the Laplace Transform of $H(t)$ gives

$$H(t) = \beta \times \left(\frac{\sinh\left(\frac{t\sqrt{(-4\alpha+m)m}}{2}\right) \mathrm{e}^{-\frac{mt}{2}} \, (-m+2\alpha)}{\sqrt{(-4\alpha+m)\,m}\,\alpha} + \frac{-\cosh\left(\frac{t\sqrt{(-4\alpha+m)m}}{2}\right) \mathrm{e}^{-\frac{mt}{2}} + 1}{\alpha} \right) \tag{19}$$

Since exponentials must be dimensionless, m is to be interpreted as a rate.

Figure 11 shows the general pattern for higher and lower cognition rates. Here, $\alpha = \beta = 1$, $m = 3/2,\ 1/6$. H_0 is the critical DRT limit from Eq.(3). The

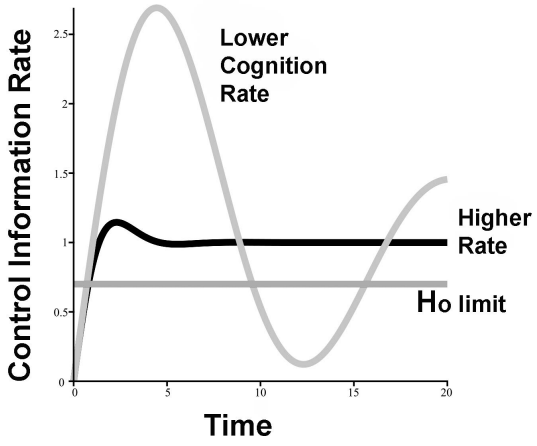

Figure 11: Control information rate $H(t)$ for the cognition rate exponential distribution having means $m = 1/6, 3/2$. $\alpha = \beta = 1$, and H_0 is the critical control information rate from the Data Rate Theorem. The system rapidly becomes grossly unstable under a low cognition rate.

system rings dangerously at the low cognition rate, while the higher rate quickly stabilizes and remains stable.

The infection model of Eq.(11), under distributed delay, becomes

$$dY(t)/dt \approx \beta + aY(t) - b\int_0^t Y(t-\tau)f(\tau)d\tau \tag{20}$$

The Laplace transform argument for the exponential distribution applied to Eq.(20) gives

$$Y(t) = \frac{\beta}{b-a} + \exp\left[(a-m)t/2\right](\cdots) \tag{21}$$

where the dotted terms within the brackets again involve sinh and cosh.

Here, in contrast to the control theory model, the essential matter is the leading exponential term $\exp[(a-m)t/2]$. If the rate of institutional cognition m is smaller than a, the average rate at which the infection spreads within the population, the outbreak explodes.

The stochastic differential equation extension of Eq.(20), which involves adding a volatility term $\sigma Y_t dW_t$, enters realms at the cutting edge of current applied mathematics which will not be pursued here (e.g., Rene and Longtin 2017).

That being said, some thought suggests that, for very high rates of institutional cognition, where the average dealy $< \tau >= \int \tau f(\tau)d\tau$ is very small, the stochastic version to Eq.(20) can be approximated as $dY_t \approx \beta - (b-a)Y_t +$

$\sigma Y_t dW_t$. Using the Ito Chain Rule, the requirement for stability in second order is then that $\sigma < \sqrt{2(b-a)}$. As $< \tau >$ increases, stability should fail at progressively smaller levels of σ.

5 Multiple delays

In reality, of course, there are often many sources of delay, affecting at least five or six critical scales and levels of organization: international, national, state/province, county, municipality, and local community or neighborhood. From the standpoint of mathematical modeling, four or more levels, it can be shown, will often require solution to quintic or higher polynomials, for which general solutions do not exist.

The additive delay version of Eq.(5) et seq. is

$$\begin{aligned} dH/dt &= \beta - \sum_{j=1}^{N} \alpha_j H(t-\tau_j) \\ H(t) &= \frac{\beta}{\sum_{j=1}^{N} \alpha_j} \left(1 - \exp[st]\right) \\ -s &= \sum_{j=1}^{N} \frac{\alpha_j}{\exp[s\tau_j]} \end{aligned} \tag{22}$$

Here, s has a negative real part only over a limited region of the τ_j centered on zero. That is, sufficiently large τ_j make $H(t)$ unstable.

For the infection model, a similar calculation involves considerably more algebra and is left as an exercise.

For the cognition rate models, matters are a little more complicated. Here, the basic relations involve the Laplace transform of $H(t)$ as

$$\begin{aligned} dH/dt &= \beta - \sum_{j=1}^{N} \alpha_j \int_0^t H(t-\tau_j) m_j \exp[-m_j \tau_j] d\tau_j \\ s\mathcal{L}(H(t),t,s) &= \frac{\beta}{s} - \left(\sum_{j=1}^{N} \frac{\alpha_j m_j}{s+m_j} \right) \mathcal{L}(H(t),t,s) \end{aligned} \tag{23}$$

Solving for, and inverting the Laplace transform $\mathcal{L}(H(t),t,s)$ gives $H(t)$ as a sum across terms in $\exp[A_j t]$, where the A_j are the solutions to a polynomial of degree $N+1$ in α_j and m_j. A_j has negative real parts only for sufficiently large cognition rates m_j.

In our 'real world', N is large, the delays are long, and cognition rates are low indeed.

Again, a similar calculation can be performed for the endemic infection model.

The Mathematical Appendix explores ways in which to extend the underlying approach.

6 Reconsidering COVID-19 dynamics

Dynamic networks are notoriously hard to stabilize. The US-Canadian power grid suffered a large-scale outage on August 10, 1996 (Rogers 2000). Figure 12a, adapted from the Rogers book, shows details of the line flow transient, power in megawatts vs. time, over about a one hundred second interval, while the grid's power control system attempted corrections of increasing amplitude until the system collapsed in a blackout. Figure 12b shows a seven day running average of the reported number of COVID-19 cases through April 29, 2021. The oscillations are again of increasing amplitude.

These are suspiciously similar to figure 8b and the low cognition rate plot of figure 11.

We have invoked national public health as a dynamic networked structure at and across various levels of governance, from the national through the state, county, and municipal levels. Response to the perturbation of an emerging infection can be indexed by the temporal dynamics of that infection. That is, infection patterns in modern states are not simply matters of host-pathogen population dynamics. They are environmental indices of underlying responses of governing networks, particularly influenced by the delay of concerted institutional response.

Let us reexamine New Zealand's COVID-19 pattern in time. Again, figure 1 shows the number of reported verified cases by day across the country, from March 1, 2020 through March 8, 2021.

The New Zealand example seems to index something quite like figure 8a: onset of heavy control, followed by minor oscillations.

The outbreaks in the USA, Brazil, England, South Africa and elsewhere – figure 2 – are quite different, as is the global example of figure 12b.

Here, we appear to see the oscillatory delay-and-lose-control dynamic of figures 11 and 8b, with increasing disease peaks as polities either fail to respond quickly, or prematurely ease social distancing restrictions, in the context of a catastrophic vaccine rollout. Recalling the 'free Michigan' tweets from the Trump White House, the compounded delay in recognition of New York City's dire circumstances at both the municipal and state levels, and the central role of New York City in the nation's urban hierarchy, this is not, perhaps, entirely unexpected.

Since New York City so strongly dominates the US urban hierarchy, public health policy in the City and State will effectively determine national patterns of the spread of infectious disease. As described, figure 4, from Wallace et al. (1999), provides a case history, showing how the New York Metropolitan Region (NYMR) drove the spread of AIDS nationally.

COVID-19 was first detected in the NYMR on March 1 and 2, 2020. Goodman (2020) describes subsequent events as follows:

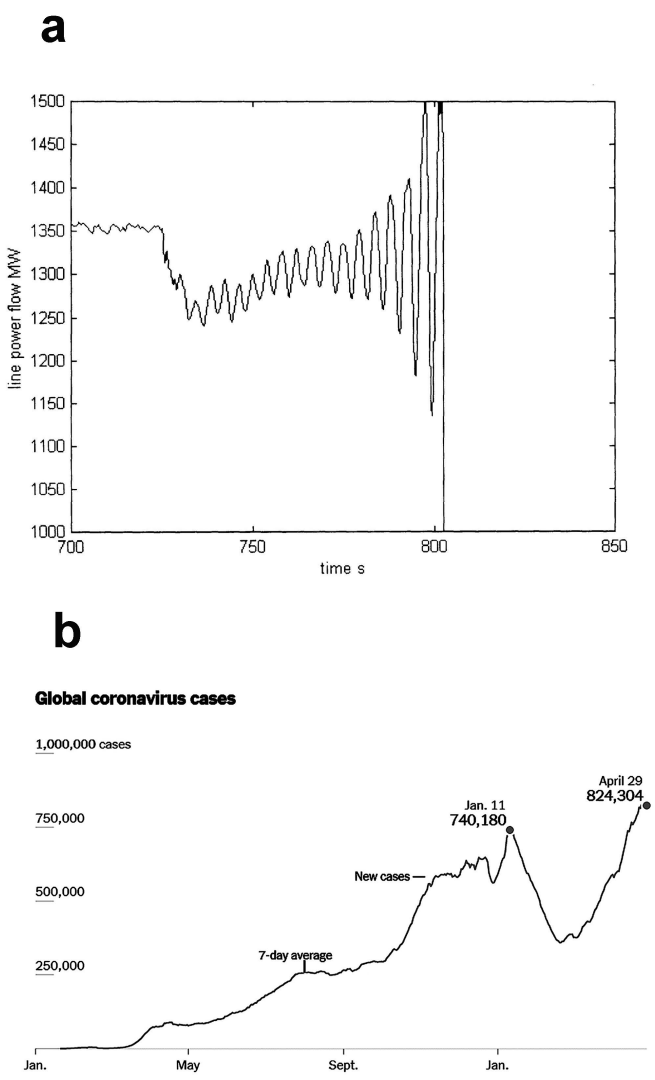

Figure 12: (a). Oscillating collapse of the US/Canadian Power Grid during the August, 1996 blackout event. The onset of increasing amplitude oscillations is characteristic of failure through critical delay in system control. (b). Adapted from the NY Times 5/1/21. A seven day running average of reported world-wide COVID-19 cases through 4/29/21. Oscillations appear to be of increasing amplitude.

> ...[T]he initial efforts by New York officials to stem the outbreak were hampered by their own confused guidance, unheeded warnings, delayed decisions and political infighting...
>
> [As former CDC Director Thomas R. Frieden put it] 'You have to move really fast. Hours and days. Not weeks. Once it gets a head of steam, there is no way to stop it.'
>
> Dr. Frieden said that if the state and city had adopted widespread social distancing measures a week or two earlier, including closing schools, stores and restaurants, then the estimated death toll from the outbreak might have been reduced 50 to 80 percent.

Goodman (2020) reports that, at a private meeting on March 12, 2020, the New York City Health Commissioner predicted 70 % of city residents could become infected if no steps were taken. Finally, City and State officials agreed to a widespread shutdown, including the closings of schools, for March 22. By then, of course, it was far too late.

The numbers from the Delayed Auditory Feedback (DAF) experiments allow perspective on the critical response time of New York City's public health establishment. The time constant for human consciousness is about 100ms, while the critical lag for DAF is about 175ms, say double. Taking Frieden's seat-of-the-pants criterion of 'Hours and days' as the time constant, as a base, then the stable zone of figure 5, where the real component is negative, is very short for New York City, certainly less than a week, understanding that as goes the City, so goes the NYMR, and, ultimately, the nation. Acting forcefully within that period, you might get some ringing nationally, but eventual convergence on zero, as suggested by figure 8a. Wait two or three weeks for plague to spread in New York City, and you get the rapidly growing amplifications of figure 8b, leading to the national pattern of figure 2. Again, see Gould and Wallace (1994) and Wallace et al. (1997, 1999) for a worked-out case history of the 'slow plague' (Gould 1993) of AIDS.

Similar stories can be written for Brazil, England, and South Africa and, apparently, globally as well.

Hours and days to control a highly contagious outbreak in the peak of the urban hierarchy. After that, national disaster.

With regard to Brazil, Castro et al. (2021) comment that

> In Rio de Janeiro, political chaos compromised a prompt and effective response. Leaders were immersed in corruption accusations, the governor was removed from office and faced an impeachment trial, and the Secretary of Health was changed three times between May and September, one of whom was arrested...
>
> ...[P]rompt and equitable responses, coordinated at the federal level, are imperative to avoid fast virus propagation and disparities in outcome.. Yet the COVID-19 response in Brazil was neither prompt nor equitable. It still isn't...

Figure 13: 'Bring out your dead'. Kingsbridge, the Bronx, in the Year of the Plague.

7 Discussion

Let us again imagine a driver on an all-night run over a poorly-maintained highway. At first, the sudden impact of a pot hole is quickly corrected: figure 7. As the drive continues, the driver begins to tire. There is now an increased delay in corrective response after hitting a bump, and the vehicle will fish-tail slightly before stabilizing: figure 8a. Toward morning, the driver is fatigued and overtired, and response rate has slowed even further, so that significant delay in correction after perturbation leads to fishtailings of increasing amplitude until the vehicle cannot remain on the road: figures 8b and 12. Cognition rate models are simpler, in a sense: take your eyes off a growing fire, and it explodes.

This is not rocket science, but it does take much effort to see beyond cultural blinders (e.g., Heine 2001) that both demand and reward focus on the population dynamics of individual-level infection rather than on the dynamics of the interlinked network of institutions tasked with the maintenance and control of public health. Those dynamics are ever and always channeled and constrained by the underlying power relations between subgroups within the polity, a matter affecting – indeed, determining – public health research funding streams. These are not dynamics that can be overcome by medical treatments of individuals, including large-scale vaccination.

Ever more complicated models of institutional pandemic control dynamics can be constructed, moving far beyond the burdens of Eqs.(5-23). The central point of such models, as the mathematical ecologist E.C. Pielou (1977) has emphasized, lies not answering questions, but in raising them for empirical and

observational study. Such study is the only possible source of new knowledge as opposed to new speculation. Mathematical and computational models are speculation, and, via Eqs.(5-23), we have explored how delays in recognition of, and response to, emerging infection is likely to trigger large-scale instabilities of a nation's disease control system, causing massively increased morbidity and mortality: figure 2 vs. figure 1.

Policy implications are clear, but solutions less so. Business community 'economic' concerns have almost always opposed early imposition of draconian disease control tactics. Messengers bearing bad news are never welcomed by the powerful, discouraging forceful statements by increasingly frantic public health authorities. Typically, egomaniacal 'dear leaders' at multiple scales of governance often denigrate expert opinion and recommendations in favor of soothing anodynes from cronies and sycophants.

Of central significance, metropolitan regions, the central agents of national and local disease diffusion according to figures 3 and 4, remain fragmented both within and between themselves regarding public health planning and authority.

New tactics are badly needed for public health strategy. Central to this is a necessary reorientation of power relations between groups. Governance must be taken from the hands of semi-demented, narcissistic 'dear leaders', their courts of crony jesters, and the many, sometimes clandestine, beneficiaries of the system who have, in fact, put them in power, and placed in the hands of the saner modalities of civil society.

A defining context for such efforts is the inevitability of spillovers much more deadly than COVID-19. These will emerge from increasingly prevalent factory farming and neocolonial, neoliberal land use policies (Wallace and Wallace 2015; Wallace et al. 2018, 2020). African Swine Fever has, at this date, killed about half the hog population in China. The hog immune system is so similar to the human that there is serious discussion of growing human organs in hogs for transplant.

As has been said in another setting, 'Winter is coming'.

Mathematical Appendix: Extending the models

Figure 3 suggests that we must, ultimately, explore spread and control of infection on a 'sociogeographic' network of linked metropolitan regions, convoluted with subordinate subnetworks of spatial contagion and social network diffusion. Sociogeographic 'space' and time then become inextricably mixed, while infection propagates across the underlying manifold at some characteristic rate c. This suggests, as in physical theory, introducing a Riemannian formalism, replacing time in the developments above with a composite index $\mathcal{S}$ written as

$$d\mathcal{S}^2 = c^2 dt^2 - \sum_j dx_j^2 \tag{24}$$

Then the defining relations subject to discrete delay become, now in $\mathcal{S}$,

$$dH/d\mathcal{S} = \beta - \alpha H(\mathcal{S} - \delta)$$
$$dY/d\mathcal{S} = aY(\mathcal{S}) - bY(\mathcal{S} - \delta) \tag{25}$$

and their distributed delay versions.

More generally, $\mathcal{S}$ should be represented via a metric tensor $\mathcal{G}$ defined by the particular underlying social structures, so that

$$d\mathcal{S}^2 \equiv \mathcal{G}_{\mu\nu} dx^{\mu} dx^{nu} \tag{26}$$

where we have introduced the usual summation convention in the indices.

Stochastic extensions of this approach are again possible, at the expense of singular mathematical complications (e.g., Herrmann 2009; Castro Villarrea 2010). We do not pursue these matters further here.

References

Abler, R., J. Adams, P. Gould, 1971, Spatial Organization: The geographer's view of the world, Prentice-Hall, New Jersey.

Ali, M., Z. Hou, N. Noori, 1998, Stability and performance of feedback control systems with time delays, Computers and Structures 66:241-248

Bailey, N., 1975, The Mathematical Theory of Infectious Diseases and Its Applications, Second Edition, Hafner Press, New York.

Bernard, S., J. Belair, M. Mackey, 2001, Sufficient conditions for stability of linear differential equations with distributed delay, Discrete and Continuous Dynamical Systems – Series II, 1:233-256.

Castro, M., S. Kim, L. Barberi, A. Riberio, S. Gurzenda ,K. Ribeiro, E. Abbott, J. Blossom, B. Rache, B. Singer, 2021, Spatiotemporal pattern of COVID-19 spread in Brazil, Science Reports doi:10.1126/science.abh1558.

Castro Villarrea, P., 2010, Brownian motion meets Riemann curvature, arXiv:1005.0650v1.

Covid Tracking Project, 2021, https://covidtracking.com/data/charts/us-currently-hospitalized.

Ferguson, N., and 29 others, 2020, Impact of non-pharmaceutical interventions (NPIs) to reduce COVID-19 mortality and health care demand. Download available from the Imperial College website.

Goodman, J.D., 2020, How Delays and Unheeded Warnings Hindered New York's Virus Fight, New York Times, April 8, July 18,

https://www.nytimes.com/2020/04/08/nyregion/new-york-coronavirus-response-delays.html

Gould, P, 1993, The Slow Plague: A Geography of the AIDS Pandemic, Blackwell, Cambridge, MA.

Gould, P., R. Wallace, 1994, Spatial structures and scientific paradoxes in the AIDS pandemic, Geografiska Annaler B 76:105-116.

Heine, S., 2001, Self as cultural product: an examination of East Asian and North American selves, Journal of Personality, 69:881-906.

Herrmann, J., 2009, Diffusion in the special theory of relativity, Physical ReviewE 80:05110.

Johns Hopkins, 2021, https://www.arcgis.com/apps/opsdashboard/index.html/bda7594740fd40299423467b48e9ecf6.

Lou, A., J. Sun, 2011, Complex Systems: Fractionality, Time-delay and Synchronization, Springer, New York.

Mao, X., C. Yuran, J. Zou, 2005, Stochastic differential delay equations of population dynamics, Journal of Mathematical Analysis and Applications, 304:296-320.

Nair, G., F. Fagnani, S. Zampieri, and R. Evans, 2007, Feedback control under data rate constraints: An overview, Proceedings of the IEEEE, 95:108137.

Newman, M., 2010, Networks: An Introduction, Oxford University Press, New York.

Nisbett, R., K. Peng, C. Incheol, A. Norenzayan, 2001, Culture and systems of thought: Holistic vs. analytic cognition, Psychological Review, 108:291-310.

Pedro, S., F. Ndjomatchoua, P. Jentsch, J. Tchuenche, M. Anand, C. Bauch, 2020, Conditions for a second wave of COVID-19 due to interactions between disease dynamics and social processes, frontiers in Physics 8: Article 574514 doi: 10.3389/fphy.2020.574514.

Pielou E.C., 1977, Mathematical Ecology, Wiley, New York.

Protter, P., 2005, Stochastic Integration and Differential Equations: A new approach, Second edition, Springer, New York.

Rene, A., A. Longtin, 2017, Mean, covariance, and effective dimension of stochastic distributed delay dynamics, CHAOS 27:114322.

Rogers, G., 2000, Power System Oscillations, Springer, New York.

Shayak, B., M. Sharma, M. Gaur, A. Mishra, 2021, Impact of reproduction number on the multiwave spreading dynamics of COVID-19 with temporary immunity: A mathematical model, International Journal of Infectious Diseases 104:649-654.

Spenser, J., 2010, The giant component: a golden anniversary, Notices of the American Mathematical Society, 57:720-724.

Wallace, D., R. Wallace, 2020, COVID-19 in New York City: An ecology of race and class oppression, Springer, New York.

Wallace, R.G., R. Wallace (eds), 2016, Neoliberal Ebola: Modeling Disease Emergence from Finance to Forest and Farm, Springer, New York.

Wallace, R., D. Wallace, H. Andrews, 1997, AIDS, tuberculosis, violent crime and low birthweight in eight US metropolitan areas: public policy, stochastic resonance and the regional diffusion of inner-city markers, Environment and Planning A 29:525-555.

Wallace, R., D. Wallace, J.E. Ullmann, H. Andrews, 1999, Deindustrialization, inner-city decay, and the hierarchical diffusion of AIDS in the USA: how neoliberal and cold war polices magnified the ecological niche for emerging infections and created a national security crisis, Environment and Planning A 31:113-139.

R. Wallace and R.G. Wallace, 2015, Blowback: new formal perspectives on agriculturally driven pathogen evolution and spread, Epidemiology and Infection, 143(SE10):2068-2080.

R. Wallace et al., 2018, Clear-Cutting Disease Control: Capital-led deforestation, public health austerity, and vector-borne infection, Springer, New York.

R. Wallace et al., 2020, Agribusiness vs. Public Health: Disease control in resource-asymmetric conflict, https://hal.archives-ouvertes.fr/hal-02513883.

Yates, A., 1963, Delayed auditory feedback, Psychological Bulletin 60:213-232.

Yi, S., P.W. Nelson and A.G. Ulsoy, 2010, Time-Delay Systems: Analysis and Control Using the Lambert W Function, World Scientific, New Jersey.

Yi, S., S. Yu, J. H. Kim, 2011, Analysis of neural networks with time-delays using the Lambert W function, Proceedings of the 2011 American Control Conference, San Francisco, CA, USA, 2011, pp. 3221-3226, doi:10.1109/ACC.2011.5991085.

Yi, S., S. Duan, P. Nelson, A. Ulsoy, 2012, The Lambert W function approach to time delay systems and the LambertW_DDE toolbox, Proceedings of the 10-the IFAC Workshop on Time Delay Systems, IFAC, doi: 10.3182/20120622-3-US-4021.00008.